Tri-Partite Assay for Studying Exon Ligation by the ai5γ Group II Intron[†]

Avital Bar-Shalom and Melissa J. Moore*

Howard Hughes Medical Institute, Department of Biochemistry, MS 009, Brandeis University, 415 South Street, Waltham, Massachusetts 02454-9110

Received April 10, 2000; Revised Manuscript Received May 30, 2000

ABSTRACT: Group II introns self-splice via a two-step mechanism: cleavage at the 5′ splice site followed by exon ligation at the 3′ splice site. The second step has been difficult to study in vitro because it is generally faster than the first. Herein we describe development and partial kinetic characterization of a novel assay for studying the second step in isolation. In this system, a truncated linear intron (nucleotides 1−881) mediates exon ligation between two oligonucleotide substrates: a 19 nt 5′ exon and a 3′ substrate consisting of the last 6 nucleotides of the intron plus a 6 nucleotide 3′ exon. We found that neither the exact structure of domain 6 nor the identity of nucleotides flanking the 3′ splice site is critical for accurate 3′ splice site choice by the ai5γ group II intron. The multiple turnover k_{cat} (0.14 min^{-1}) is slower than the single turnover k_{obs} (0.6−0.7 min^{-1}), consistent with rate-limiting product release under steady-state conditions. Decreased single turnover rates at lower pHs were more consistent with loss of catalytic activity than with rate-limiting chemistry. Binding of the 3′ substrate ($K_m = 2.6\ \mu$M) could be improved by changing a long-range A:U base pair involving the last intronic nucleotide (the $\gamma-\gamma'$ interaction) to G:C ($K_{m(3'\ substrate)} = 1\ \mu$M).

Group II introns are widely dispersed transposable elements found in mitochondria, chloroplasts, and bacteria (*1*−*3*). All introns of this class share a common secondary structure consisting of six domains emanating from a central wheel [Figure 1A (*1*, *2*)]. Excision of these introns occurs by the same two-step mechanism as nuclear pre-mRNA splicing (*4*−*6*), but in vitro, many group II introns can mediate their own removal without the aid of proteins (*7*, *8*). Because the chemistry of group II introns and nuclear pre-mRNA splicing is identical, group II introns are widely believed to be evolutionary precursors to spliceosomes (*9*, *10*). Also, group II introns are the only known natural RNA catalysts that mediate multiple reactions having products with distinctly different structures (i.e., branched vs linear species).

The splicing pathway for group II introns (Figure 1B, left) was initially established from studies of the fifth intron of the *Saccharomyces cerevisiae* mitochondrial cytochrome oxidase gene (ai5γ; *7*, *8*) and the first intron of the apocytochrome b gene (bI1; *11*). In the first step, the 2′-hydroxyl (2′-OH) of a bulged adenosine in domain 6 attacks the 5′ splice site, releasing the 5′ exon and forming a lariat intermediate containing a 2′-5′ phosphodiester bond between the branch site adenosine and the first intronic nucleotide. In the second step, the free 3′-OH of the 5′ exon attacks the 3′ splice site, releasing the intron (lariat product) and ligating the exons (*6*). The first step of splicing can also occur via hydrolysis at the 5′ splice site [Figure 1B, right (*12*−*14*)]. The 5′ exon and linear intron-3′ exon then undergo exon ligation as above to release a linear intron product and ligated exons. An additional reaction catalyzed by group II introns under certain salt conditions in vitro is spliced exon reopening to yield free 5′ and 3′ exons (*12*, *15*, *16*).

The most extensively studied group II intron to date is ai5γ (*17*, *18*). The elements critical for cleavage at the 5′ splice site are well understood. The 5′ exon contains two intron binding sites, IBS1 and IBS2, complementary to exon binding sites EBS1 and EBS2 in domain 1 (Figure 1A). Base pairing between these sequences is crucial for accurate 5′ splice site definition (*19*) and prevents dissociation of the 5′ exon from the intron after cleavage (*20*). Precise 5′ splice site identification is enhanced by two base pairs between intron positions 3 and 4 (ϵ) and an unpaired region in stem C1 of domain 1 [ϵ' (*21*)]. Domain deletion studies (*22*) and development of a minimal trans assay that monitors 5′ splice site cleavage (*23*) revealed that only domains 1 and 5 are necessary for 5′ splice site hydrolysis. However, branch formation additionally requires domain 6 since it contains the bulged branch site adenosine (*22*, *24*).

The mechanisms and interactions involved in 3′ splice site selection are not as well understood. One reason for this is that the second step of splicing by the ai5γ intron is significantly faster than the first (*15*, *20*), therefore the effects of sequence alterations that might affect exon ligation are often masked. Still, some second step requirements have been elucidated. Alteration of the number of nucleotides between domains 5 and 6 or a complete deletion of domain 6 activated numerous cryptic exon ligation sites to either side of the natural 3′ splice site (*22*, *25*). In the context of a domain 6 deletion, exon ligation depends on two long distance base-pairing interactions, $\gamma-\gamma'$ and $\delta-\delta'$, between intronic nucleotides A587 and U328 and nucleotides U887 and A+1,

* To whom correspondence should be addressed. Phone: (781) 736-2359. Fax: (781) 736-2337. E-mail: mmoore@brandeis.edu.

† This work has been supported by the Howard Hughes Medical Institute, NIH Grant GM53007-05 (M.J.M.), and NIH training Grant GM07596 (A.B.).

10.1021/bi000808w CCC: $19.00
Published on Web 07/26/2000

the bases on either side of the 3′ splice site, respectively [Figure 1A (*19*, *21*)]. Modification interference assays have shown that the tip of domain 6, a GUAA tetraloop, is involved in an interaction (called $\eta-\eta'$) with domain 2 that plays a role in a conformational change occurring between the first and second steps of splicing (*26*). Recently, bi-partite assays consisting of free 5′ exon plus linear or lariat intron-3′ exon intermediate were used to specifically probe the effects of a phosphorothioate substitution at the 3′ splice site (*27*, *28*) and various divalent metal ions on exon ligation (*29*).

Our goal was to develop an assay for studying in isolation the molecular interactions required for 3′ splice site recognition and exon ligation by the ai5γ group II intron. For these purposes, it was desirable to both bypass the first step of splicing (for reasons noted above) and provide the 3′ splice site on a separate molecule from the remainder of the intron. The benefit of creating such a tri-partite system is that it should allow us to determine the extent to which various 3′ splice site modifications affect binding/recognition versus the catalytic rate. Moreover, both single and multiple turnover kinetic studies can be performed.

Here, we report partial kinetic characterization of both bi-partite (Figure 1C, left; free 5′ exon and linear intron-3′ exon) and tri-partite (Figure 1C, right; 5′ exon, linear intron, and 3′ splice site substrate) assays for exon ligation. The former was used to determine saturating conditions for the 5′ exon, as well as examine the physical basis for the biphasic kinetics often observed for the ai5γ intron. Development of the tri-partite assay has yielded novel information about the extent to which domain 6 can be modified without sacrificing accurate exon ligation, as well as a subset of interactions involving nucleotides flanking the 3′ splice site that contribute to active site binding.

Table 1: 5′ Exon and 3′ Substrate Sequences[a]

RNA substrate	sequence
5′ exon	GGAGUGGUGGGACAUUUUC
3′ substrate A	AAAGGUCUACCUAUCGGGAU/ACUAUG
3′ substrate B	GUCUACCUAUCGGGAU/ACUAUG
3′ substrate C	CCUAUCGGGAU/ACUAUG
3′ substrate D	UCGGGAU/ACUAUG
3′ substrate E	CGGGAU/ACUAUG
3′ substrate F	GGGAU/ACUAUG
3′ substrate G	GGAU/ACUAUG
3′ substrate H	GAU/ACUAUG
3′ substrate I	AGGUCUACCUAUCGGGAU/ACUAUG
3′ substrate E γ'U→C	CGGGAC/ACUAUG
3′ substrate E δ'A→G	CGGGAU/GCUAUG
3′ substrate E γ'U → C, δ'A→G	CGGGAC/GCUAUG

[a] For each 3′ substrate, a slant (/) indicates the 3′ splice site.

EXPERIMENTAL PROCEDURES

Plasmids. Plasmid pJD20 (*12*) was generously provided by Anna Marie Pyle. Plasmids derived from pSP64 (*30*) that contain point mutations at the δ [Δ52/328C (*19*)] and γ [Δ13/587G (*21*)] positions were generous gifts from Alain Jacquier. A pSP64 derivative in which both the δ and γ were mutated (Δ52/328C, 587G) was created by cloning the 677 nt SnaBI/EcoRI fragment from Δ13/587G into similarly digested Δ52/328C vector.

Transcription Templates. Transcription templates were created by PCR amplification (*31*) of the above plasmids. The upstream primer provided a T7 RNA polymerase promoter immediately upstream of G1 of the intron. Downstream primers generated PCR products containing a 190 nt 3′ exon or desired truncations within domain 6.

RNA Transcription. Intron-containing RNAs internally labeled with [α-^{32}P]UTP (10μCi/μL, NEN) were transcribed (*32*) and purified by denaturing PAGE (4%; 29:1). These transcription reactions also contained GMP at 4-fold excess over GTP to generate 5′-monophosphate ends. Concentrations of purified transcripts were calculated from the specific activity of the transcription reaction and the number of uridines in the transcript. Larger quantities of unlabeled RNAs were generated according to a transcription protocol provided by Zvi Pasman (Pers. comm.). These reactions contained 6 mM $MgCl_2$, 40 mM Tris-HCl pH 8.1, 1 mM Spermidine, 5 mM DTT, 0.01% Triton X-100, 80 μg/mL PEG 8000 (*33*), 10 mM $MgCl_2$, 2 mM each ATP, CTP, and UTP, 1 mM GTP, 6 mM GMP, 80 μg/μL of DNA and 1 unit/μL T7 RNA polymerase (Stratagene, 50 unit/μL). Each reaction was divided into several tubes (no more than 200 μL/tube) and incubated at 37 °C. After 10 min, 1 μL of pyrophosphatase (USB, 40 unit/mL) was added and 37 °C incubation continued for 2 h. Subsequent RNA purification was as above, except that RNA was visualized by UV shadowing and quantified spectrophotometrically, using 1 OD (at 260 nm) = 40 μg/mL. Ribozymes in Figures 6 and 7 were transcribed similarly except that trace quantities of [α-^{32}P]UTP were added to facilitate quantification. For these ribozymes, free nucleotides were removed with a Sephadex G-50 (Amersham Pharmacia) spin column, then the RNA was extracted and precipitated; no further purification was performed.

RNA Oligonucleotide Sequences and Labeling. RNA oligonucleotides (Table 1) were synthesized on an Expedite oligonucleotide synthesizer, deprotected according to manufacturers' directions (Glen Research or Millipore) and gel purified. The 3′ splice site substrates were generally 5′-monophosphorylated by incubating 1−10 nmol of RNA with T4 polynucleotide kinase (5−20 units, Promega) and excess cold ATP. For radiolabeled RNAs, [γ-^{32}P]ATP (150 μCi/μL, NEN) was added at 1/10 the unlabeled ATP concentration. Single label incorporation onto the 3′ exon (3′ labeling) was accomplished by attaching a 5′-[^{32}P],3′-bisphosphate cytidine (ICN) with T4 RNA ligase (*34*).

Splicing Reaction Conditions. All solutions were prepared with DEPC[1]-treated water and sterile filtered or autoclaved. Reactions were performed in volumes of 10−40 μL. For each reaction, RNAs were combined in a 1.5 mL tube with MOPS (Sigma, minimum 99.5%), pH 7.5, and heated at 90 °C for 1 min, then transferred to a 45 °C water bath to equilibrate. $(NH_4)_2SO_4$ and $MgCl_2$ were combined and pre-warmed to 45 °C. Reactions were initiated by addition of salts im-

[1] Abbreviations: DEPC, diethylpyrocarbonate; E1dC, 5′ exon with a 3′ deoxy-cytidine; EBS, exon binding site; fp, fraction product; HEPES, *N*-[2-hydroxyethyl]piperazine-*N*′-[2-ethanesulfonic acid]; IBS, intron binding site; LI-3′ exon, linear intron-3′ exon; MES, 2-[*N*-morpholino]ethanesulfonic acid; MOPS, 3-[*N*-morpholino]propanesulfonic acid; nt(s), nucleotide(s); PCR, polymerase chain reaction; PIPES, piperazine-*N*,*N*′-bis[2-ethanesulfonic acid].

mediately before taking timepoints. Final concentrations were 40 mM MOPS, pH 7.5, 0.1 M $MgCl_2$, and 0.5 M $(NH_4)_2SO_4$.

Bi-Partite Kinetics. Reactions containing 0.1 nM linear intron-3′ exon and 50−700 nM 5′ exon were followed for 30 min (reactions below 50 nM 5′ exon were not included since a cryptic cleavage product complicated the quantification). Aliquots (3 μL) were removed at set times and quenched with 10 M urea, 1× TBE loading buffer, and kept on ice. Products were separated by electrophoresis in a denaturing 4% (29:1) polyacrylamide gel, which was subsequently analyzed by phosphorimaging (Molecular Dynamics). The extent of reaction was determined by summing the intron product, ligated exons and free 3′ exon and dividing by the total amount of reactants and products in each lane. The product fraction was then plotted versus time. The data fit best to a double exponential equation: fp (fraction products) $= k_1 + [k_2(1 - e^{(-k_3t)})] + [k_4(1 - e^{(-k_5t)})]$ where $k_1 = y$-intercept, $k_2 =$ amplitude (fraction) of the fast phase, $k_3 =$ rate of the fast phase, $k_4 =$ amplitude of the slow phase, $k_5 =$ rate of the slow phase, and $t =$ time. Each concentration time course was repeated three times to calculate an average rate for the fast phase. These average rates were then used to determine K_{app} and k_{obs}.

Tri-Partite Exon Ligation Assays. Experiments to determine efficacy of exon ligation in the context of a nicked domain 6 were performed with a 5′-labeled 3′ substrate (50 nM plus 10 μM intron and 15 μM 5′ exon) or 3′-labeled 3′ substrate (5 nM plus 15 μM intron and 15 μM 5′ exon). Reactions shown in Figures 3B, 5A, and 7 were separated in 25% (19:1, 1 M urea) denaturing polyacrylamide gels; reactions in Figure 3C were separated in a 20% (19:1) denaturing polyacrylamide gel. Products were visualized and quantified as in the bi-partite assay. For single turnover kinetics (Figure 5), reactions were performed with 20 μM 5′ exon, 200 nM to 1.5 μM ribozyme (intron nucleotides1−881), and 10 nM 5′-^{32}P-labeled 3′ substrate. Reaction products were analyzed on a 25% (19:1) 1 M urea denaturing polyacrylamide gel and quantified by phosphorimaging. A graph of the data best fit the single-exponential equation: fp $= k_1 + [k_2(1 - e^{(-k_3t)})]$ where $k_1 = y$-intercept, $k_2 =$ extent of reaction, $k_3 =$ reaction rate, and $t =$ time. K_m and k_{cat} determinations for the tri-partite assay were performed with the 5′ exon at saturation (15−20 μM), 10 nM ribozyme, and 0.1−6 μM 5′-^{32}P-labeled 3′ substrate. Experiments which monitored both burst and steady-state kinetics as a function of pH contained 15 μM each 5′ exon and 3′ substrate plus 1 μM ribozyme. The data best fit an equation that described the fast phase (single exponential) plus a linear phase (the steady-state): fp $= k_1 + [k_2(1 - e^{(-k_3t)})] + k_4t$, where $k_4 =$ the rate of the steady-state reaction and other constants are as above. pH-rate profiles were performed in 20−40 mM MES, MOPS, PIPES, or HEPES at appropriate pHs.

Mutation Studies. Single turnover conditions were used to test the $\gamma-\gamma'$ and $\delta-\delta'$ long-range base pairs with wild-type and mutant ribozymes and 3′ substrates as noted (Figure 7). Reactions containing 20 μM 5′ exon and the indicated ribozyme (nts 1−881), 100 nM indicated 3′ substrate and 40 mM MOPS, pH 7.5 were followed for a maximum of 30 s. K_m and k_{cat} determination for the $\gamma-\gamma'$ G:C combination were performed as above for the wild-type pair.

RESULTS

Choice of Substrates and Assay Conditions. The components of the second step of splicing consist of a free 5′ exon and either a linear or lariat intron-3′ exon intermediate (Figure 1B). We chose to begin characterizing the kinetics of exon ligation using the linear intron-3′ exon intermediate because it is simpler to prepare, and splicing by 5′ splice site hydrolysis is a relevant pathway in vivo (*27*). Initially, we determined the kinetic parameters for a single turnover bi-partite assay (Figure 1C, left) in which an unlabeled 5′ exon (19 nts; Table 1) was added to a radiolabeled, gel-purified transcript (LI-3′ exon, 1077 nts) consisting of the 887 nt intron plus a 190 nt 3′ exon. The 5′ exon is identical to that in the E1a −19/8 substrate used by Michels and Pyle (*23*) for kinetic characterization of 5′ splice site hydrolysis. The 5′ exon contains two sequences (intron binding sites IBS1 and IBS2) that base pair with complementary sequences (exon binding sites EBS1 and EBS2) within domain I [Figure 1A (*20*)]. The length of the 3′ exon was chosen as 190 nts so that the intron-3′ exon, intron product, ligated exons, and free 3′ exon could all be visualized on the same gel.

Splicing of the ai5γ intron has been reported in a variety of salt and buffer conditions (see, for example, refs *17*, *18*, *28*, and *29*). While similar, the conditions differ in buffer type, pH, and monovalent salts. In our hands, the conditions that gave the most efficient splicing of full-length constructs with the least RNA degradation were 40 mM MOPS, pH 7.5, 0.1 M $MgCl_2$, and 0.5 M $(NH_4)_2SO_4$ [data not shown (*35*)]. Splicing of the full-length ai5γ intron shows a sharp temperature optimum at 45 °C (*7*), and this temperature has been used in most studies of 5′ splice site hydrolysis and branch formation (*16*, *23*, *24*, *29*, *36*). When we examined the effect of temperature on bi-partite exon ligation, the fraction of LI-3′ exon reacting in the rapid phase (see below) was highest at 45 °C (data not shown). Therefore we chose these conditions to begin kinetic analysis of exon ligation.

Characterization of the Bi-Partite Exon Ligation Assay. A typical time course for the bi-partite exon ligation assay is shown in Figure 2A. As radiolabeled LI-3′ exon disappears, both linear intron and ligated exons appear simultaneously. Subsequently, free 3′ exon is produced by the spliced exon reopening reaction [see Figure 1B (*12*)]. Both the ligated exon and free 3′ exon products appeared as doublets. However these doublets do not result from splice site infidelity because digestion of purified ligated exon product with RNase T_1 yielded a single band spanning the splice junction (data not shown). Thus, the doublets likely reflect 3′ end heterogeneity produced by T7 RNA polymerase during transcription (*37*, *38*).

When we initiated these studies, no kinetic parameters had been reported for any second step assay. We observed that the rate of product appearance over time was best fit by a double exponential equation (Figure 2B; see Experimental Procedures for equation) with an initial fast phase accounting for ca. 60% of the product. This type of behavior was previously proposed to reflect the presence of alternate intron conformations (see Discussion). To test this hypothesis, we allowed a bi-partite exon ligation reaction to reach the slow phase, then quickly denatured the ribozyme at 90 °C and returned it to 45 °C to allow the reaction to proceed. This treatment resulted in a second fast phase followed by a slow

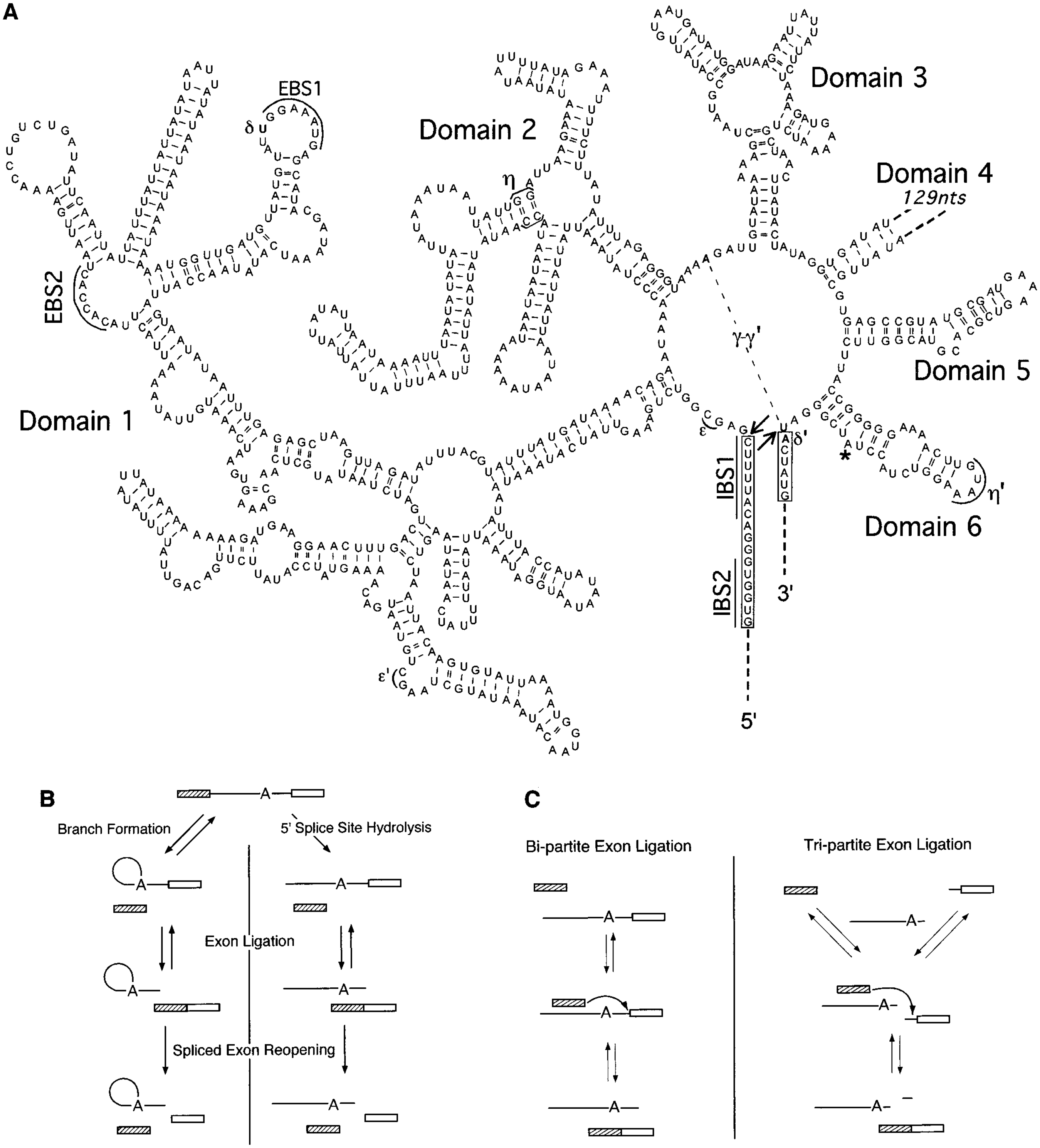

FIGURE 1: Structure of and reactions catalyzed by the ai5γ group II intron. (A) A schematic secondary structure of the ai5γ group II intron. Six domains make up the secondary structure of the intron, separating the 5′ and 3′ exons (in boxes; arrows indicate splice sites). A subset of the known long distance interactions are labeled, including $\epsilon-\epsilon'$, $\eta-\eta'$, EBS1, and EBS2 in domain 1 that interact with IBS1 and IBS2, respectively, in the 5′ exon, and the $\gamma-\gamma'$ and $\delta-\delta'$ (bold) base pairing interactions around the 3′ splice site. The branch site is marked by an asterisk. Adapted with permission from (*26*). (B) In vitro splicing reactions observed for the ai5γ intron. Alternate pathways differ in the first step only, either branch formation (left) or 5′ splice site hydrolysis (right). Spliced exon reopening is a reaction commonly observed in vitro. Hatched boxes represent 5′ exon, straight lines (with an A) represent linear introns, circles with a straight tail are lariats, and either form of the intron attached to a box is an intron-3′ exon. (C) Schematics of the two assays used here to study exon ligation. (Left) Bi-partite exon ligation mimics the second reaction of the hydrolysis pathway diagrammed in panel B and allowed determination of the binding constant for the 5′ exon. (Right) Tri-partite exon ligation. A short line attached to a box is the 3′ splice site substrate.

phase with similar proportions as the initial reaction (Figure 2C). We therefore conclude that the two phases do reflect alternate conformational states of the intron. We tried a number of folding and reaction regimens to increase the proportion of intron reacting in the fast phase but never observed a fast fraction of more than 65% (data not shown). For all subsequent experiments with the bi-partite assay, we limited our analyses to the fast phase.

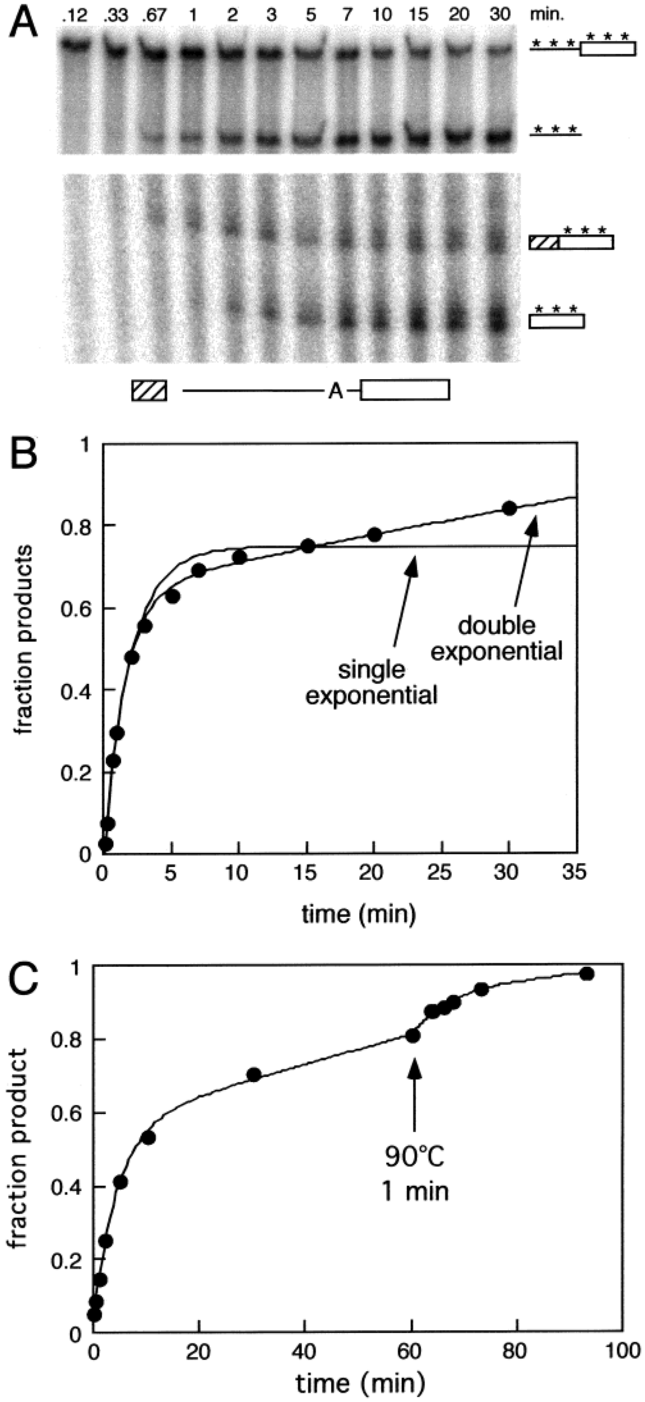

FIGURE 2: The bi-partite exon ligation assay displays biphasic kinetics. (A) Phosphorimage of a denaturing polyacrylamide gel showing that labeled linear intron-3′ exon disappears over time as ligated exons and intron product appear. Subsequent spliced exon reopening gives rise to free 5′ and 3′ exons, of which only the labeled 3′ exon is visible [(*) radiolabel]. Exon product doublets can be attributed to 3′ end heterogeneity (see Results). (B) Plot of fraction products versus time fit to both single and double exponential equations. The fraction product at each time point was taken as the sum of the linear intron product, ligated exons and free 3′ exon divided by the total of all four species. The data fit the following equation: fraction products (fp) $= -0.031 + \{0.67[1 - e^{(-0.65t)}]\}$. (C) To test whether the slow phase represented a different intron conformer, a time course was followed until it reached the slow phase, the RNAs were then heat denatured, and further timepoints taken at 45 °C.

Exon ligation in the bi-partite assay obeyed saturation kinetics with K_{app} for the 19 nt 5′ exon of 50 ± 9 nM and a maximum observed rate (k_{obs}) of 0.6 ± 0.2 min^{-1} (data not shown). Consistent with a previous report (*28*), we found that the rate of exon ligation in the bi-partite assay showed no dependence on pH in the range from 6.0 to 8.0 (data not shown). Thus, the catalytic step is not rate-limiting in this assay (*39*).

Development of a Tri-Partite Assay for Exon Ligation. Having determined a K_{app} for the 5′ exon, the next step in development of a tri-partite exon ligation assay was to truncate the intron so that the 3′ splice site could be provided on a separate molecule (3′ substrate) from the catalytic core. Ideally the intron should retain the branch site to allow for possible future studies of lariat structure on 3′ splice site recognition and exon ligation. However, we faced two unknowns: (1) whether accurate exon ligation required a completely intact phosphodiester backbone in domain 6, and (2) the minimum number of base pairs within domain 6 required for binding and accurate positioning of the 3′ splice site.

To test whether nicks could be introduced into domain 6 downstream of the branch site, we transcribed a series of introns truncated at nucleotides 880, 881, 882, 883, and 884. These were individually combined with an appropriate oligonucleotide partner (3′ substrate) that supplied the remainder of the intron plus a six nucleotide 3′ exon (Figure 3A, constructs D−H). Initially, reaction at the 3′ splice site was followed by monitoring cleavage of 5′-[^{32}P]monophosphorylated 3′ substrates (Figure 3B). When combined with an excess (10 μM) of the appropriate intron and saturating 5′ exon (15 μM), all five 3′ substrates (50 nM) were cleaved, although to different extents. This cleavage occurred primarily at the wild-type 3′ splice site. By 30 min, cleavage of substrates D and E was essentially complete (91 and 94% reacted, respectively). Substrate F was significantly less reactive (15% cleavage at 30 min), and substrates G and H were minimally reactive (0.2 and 0.4% cleavage at 30 min, respectively). In the gel shown, small quantities of products were observed for both substrates D and E that likely resulted from cryptic cleavage at the phosphodiester bonds immediately adjacent to the wild-type 3′ splice site (Figure 3B, lanes 1−6; faint bands above and below main cleavage product). However, in many other reactions with these same substrates, these cryptic cleavage products were undetectable (data not shown). Therefore, we conclude that accurate reaction at the 3′ splice site can occur in the context of a nicked domain 6.

It was next necessary to determine whether the observed intronic cleavage product was produced by exon ligation, 3′ splice site hydrolysis or a combination of the two. Under the above reaction conditions, all intronic cleavage products decreased significantly or disappeared completely when the 5′ exon was omitted (Figure 3B, lanes 10−18 and 25−30). The small amount of intronic product observed for substrates D and E in the absence of the 5′ exon (lanes 12 and 15) did indicate a low level of 3′ splice site hydrolysis. However, the extent of reaction under these conditions was only 0.2−0.5% that observed when the 5′ exon was present.

To confirm that exon ligation was occurring when the 5′ exon was available, we used 3′-end labeled substrate E to allow detection of ligated exon product (Figure 3C). When this substrate was incubated with excess intron E and saturating 5′ exon (lane 1), both ligated exons and free 3′

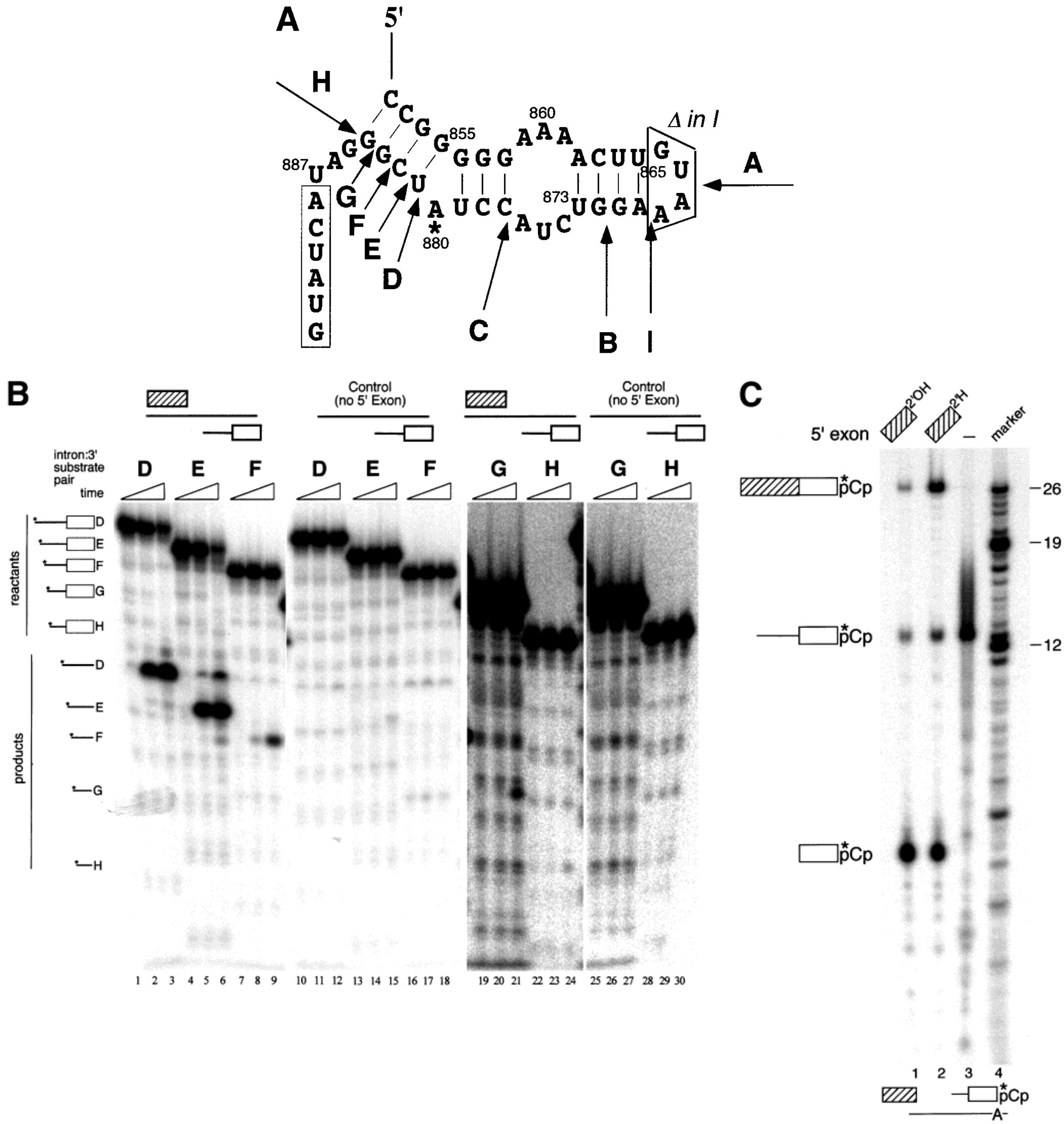

FIGURE 3: Development of a tri-partite assay for exon ligation. (A) Arrows indicate sites (A−H) in domain 6 where nicks (see text) were introduced to separate the 3′ splice site from the remainder of the intron (Table 1). Intron:3′ substrate pair I deletes the tetraloop at the tip of domain 6. (B) Tests of intron:3′ substrate pairs with nicks downstream of the branch site. Single turnover reactions containing 50 nM 5′ end-labeled 3′ substrates (D to H) and 10 μM of the appropriate linear intron with (lanes 1−9, 19−24) or without (lanes 10−18, 25−30) 15 μM free 5′ exon were followed for 0.1, 5, or 30 min. All panels are from the same gel; lanes 19−30 are from a darker exposure. Migration positions for labeled substrates and intronic oligonucleotide cleavage products are indicated to the left. (C) Oligonucleotide substrate E was radiolabeled at the 3′ terminus (see Experimental Procedures) to allow detection of ligated exons and free 3′ exon when combined with intron E (15 μM) and free 5′ exon (15 μM, 60 min, lane 1) or 5′ exon terminating with a 2′-deoxy cytidine (15 μM, 97 min, lane 2). Lane 3 contains unreacted 3′ substrate E. Substrates and products are labeled to the left; asterisk denotes ^{32}P label.

exon were observed. When the same reaction was carried out with a 5′ exon containing a 3′-terminal 2′-deoxy-cytidine (lane 2), ligated exons represented a greater proportion of the products. This is consistent with other reports and our own observations that if the 5′ exon terminates with a 2′-deoxy sugar, the spliced exon reopening reaction (Figure 1B) is slowed significantly (data not shown, ref *28*). This suggested that most of the free 3′ exon in lane 1 was produced by spliced exon reopening. However, it was also possible that the 5′ exon activated 3′ splice site hydrolysis in the tri-partite assay. To rule out this possibility, we tested whether 5′-^{32}P-labeled substrate E was cleaved in the presence of intron E and a 5′ exon having a 2′,3′-dideoxy 3′ terminus. Although the 3′-OH of the 5′ exon is required for

A

Intron:3′ Substrate	Extent of Reaction
A:A	+
B:B	+
C:C	++
D:D	+++
E:E	+++
F:F	+
G:G	+/-
H:H	+/-
I:I	++
E:A	+
E:B	+
E:C	+

B

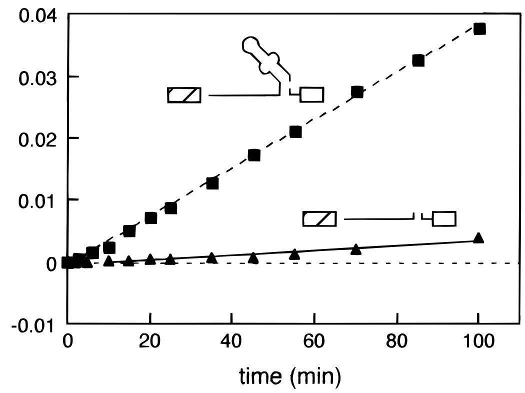

FIGURE 4: Effects of domain 6 structural changes exon ligation. (A) Further tests on various intron:3′ substrate pairs revealed that all were reactive to some degree. Intron E also cleaved substrates A−C which provided 14, 10, and 5 nts of overlapping sequence to the intron. (B) 3′ substrate E was combined either with a linear intron terminating at nucleotide 881 (to create a nicked but otherwise intact domain 6) or one terminating at nucleotide 854 (see Figure 3A) to generate a truncated domain 6 consisting of only three base pairs. Under multiple turnover conditions (20 μM 5′ exon, 100 nM ribozyme, and 10 μM substrate E), the construct with the truncated domain 6 (▲) formed products 10 times more slowly than that containing a complete, but nicked domain 6 (■). The dotted line indicates zero product. Equations used to fit the data were fp $= -0.000\,53 + (3.9 \times 10^{-5})t$ (▲) and fp $= -0.000\,64 + 0.00039t$ (■).

exon ligation (it is the nucleophile), this group should not be required for 3′ splice site hydrolysis. The 2′,3′-dideoxy 5′ exon induced no cleavage of substrate E, even though it is a competitive inhibitor of exon ligation (data not shown). Taken together, all of the above results indicate that the vast majority of the intronic cleavage product observed in the tri-partite assay must result from exon ligation; subsequent reopening of the spliced exons leads to evolution of free 3′ exon.

Majority of Domain 6 Is Dispensable for Exon Ligation. In the course of developing the tri-partite assay, we also tested several other structural permutations of domain 6. Intron:3′ substrate pairs that introduced nicks 3′ to nucleotides 867, 871, and 875 (constructs A−C in Figure 3A) were all active in a 3′ substrate cleavage assay (similar to the experiment shown in Figure 3B; data not shown). We also found that an intron:3′ substrate pair that removed the domain 6 tetraloop (i.e., the intron terminated at position 865 and the 3′ substrate initiated at position 870; Figure 3A, construct I) was active (data not shown). However, none of these pairs was as active as either construct D or E (Figure 4A). We also tested the effects of adding extra nucleotides to domain 6. Intron E (terminating at position 881; see Figure 3A) was combined with 3′ substrate A, B, or C to produce domain 6 hybrids containing 5, 9, or 14 additional overlapping nts. All of these combinations exhibited accurate 3′ splice site cleavage, but again to a lesser extent than constructs D or E (data not shown; Figure 4A).

It had previously been reported that a complete deletion of domain 6 still allows some exon ligation in a cis splicing construct, although with reduced splice site fidelity (*22*). To test the effects of eliminating most of domain 6 in our assay, we combined 3′ substrate E with an intron that terminated at nucleotide 884 to generate a truncated domain 6 comprising just a 3 nucleotide stem. This intron:3′ substrate pair produced an accurate oligonucleotide cleavage product at the 3′ splice site in the tri-partite exon ligation assay (data not shown), although at a rate ca. 10-fold slower than the tri-partite system that reconstructed a complete domain 6 (Figure 4B).

Kinetics of Tri-Partite Exon Ligation. To initiate kinetic characterization of the tri-partite exon ligation assay, we chose intron:3′ substrate pair E (Figure 3A) because this pair coupled high activity with potential maintenance of a bulged branch site adenosine in the intron. All reactions were performed with the assay consisting of free 5′ exon at saturation (15−20 μM). A single turnover intron E (hereafter referred to as the ribozyme) in excess of 5′-end labeled 3′ substrate E resulted in rapid substrate disappearance as intron cleavage product appeared (Figure 5A). In contrast to the biphasic nature of the bi-partite assay (Figure 2B), these data were best fit by a single exponential equation (Figure 5B). This suggested that only one ribozyme conformer contributed to the observed rate of exon ligation. In a series of time courses where the 3′ substrate was held constant (10 nM) and the intron concentration was varied between 0.2 and 1.5 μM, the initial rate was observed to increase linearly with intron concentration. Thus k_{obs}/K_{app} conditions prevailed in these reactions (slope $= k_{obs}/K_{app} = 0.27\ \mu M^{-1}\ min^{-1}$; Figure 5C). Interestingly a linear fit of the data in Figure 5C has a positive *y*-intercept. This suggests that this single-turnover assay may best be described by a second or higher order rate equation (*40*).

Because the amount of gel-purified ribozyme we could generate became limiting, we were unable to determine k_{obs} and K_{app} for the single turnover assay directly. Therefore we turned to multiple turnover conditions to establish a K_m for the 3′ substrate. The rate of these reactions proceeded linearly, with the ribozyme undergoing up to 15 turnovers (data not shown). This assay obeyed Michaelis−Menten kinetics with a $K_m = 2.6 \pm 1.1\ \mu M$ for the 3′ substrate and $k_{cat} = 0.14 \pm 0.03\ min^{-1}$. Using this K_m as an approximation of K_{app} under single turnover conditions, we can estimate the single turnover k_{obs} above to be ca. 0.70 min^{-1}. Since k_{cat} is slower than the estimated k_{obs}, product release may be rate-limiting under multiple turnover conditions.

pH Rate Profiles. We next wanted to establish conditions where the nature of the rate-limiting step was known. If the rate-limiting step of a reaction involves a single proton transfer, then the observed rate should have a log-linear dependence on pH with a slope near 1.0 (*39*). Such a relationship between rate and pH is often interpreted to indicate that chemistry may be rate-limiting under such assay conditions (*28*, *29*, *41*).

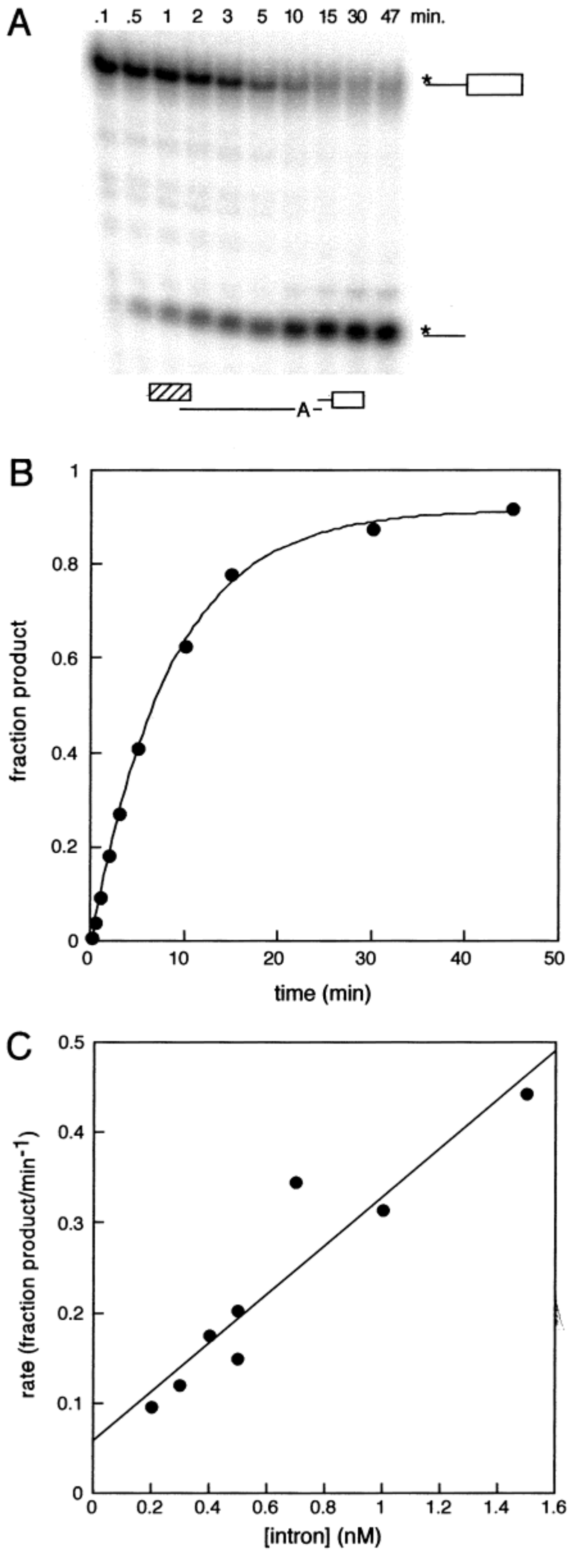

FIGURE 5: Tri-partite kinetics under single turnover conditions. (A) Time course showing rapid disappearance of the 3′ substrate (10 nM) and appearance of intronic oligonucleotide cleavage product ([5′ exon] = 20 μM, [ribozyme] = 300 nM). (B) A plot of fraction product versus time fits a single-exponential equation: fp = −0.075 + 0.95(1 − $e^{-0.15t}$). (C) Initial rates from a series of time courses versus intron concentration display a linear correspondence {rate = 0.058 + (0.271[intron])}.

To examine the effects of pH on the rate of the tri-partite exon ligation assay, we followed a series of time courses where both the all-ribo 5′ exon and wild-type 3′ substrate E were saturating (15 μM), the ribozyme was 1 μM, and the pH was varied from 5.5 to 8.1 (Figure 6). For these reactions, the ribozyme was transcribed and purified over a size exclusion column to remove unincorporated nucleotides and abortive transcription initiation products. This procedure yielded more RNA per transcription reaction, enabling us to perform multiple time courses with high ribozyme concentrations. The high ribozyme concentrations in turn allowed us to observe the burst of product formed in the initial turnover, as well as the subsequent steady state. Therefore, we could monitor the effects of pH on both the single and multiple turnover rates, as well as the fraction of product produced in the burst phase. We also measured the rate of exon ligation under these conditions using a 5′ exon terminating with a deoxy-C (E1dC). Consistent with previous reports (*28*, *29*), exon ligation was substantially slowed by this modification to the point where we could only monitor the rate of the first turnover (data not shown).

With the all-ribo 5′ exon, burst kinetics were observed at all pHs tested. Data from each time course were fit with an equation describing a single exponential (the burst phase) plus a line (the steady-state rate) (see Materials and Methods; Figure 6A). Both the single turnover and steady-state rates decreased with pH with slopes nearest 1.0 in the range from pH 5.5 to 6.0 (Figure 6B). The rate of exon ligation with the E1dC 5′ exon behaved similarly. However, we also observed a marked decrease in the amplitude of the burst phase of the all-ribo reactions in this pH range (Figure 6, panels A and C). This suggests that a smaller fraction of ribozyme is active at these pHs, which could readily account for the observed rate decreases (see Discussion). Thus we did not pursue further kinetic characterization of any tri-partite reaction at low pH.

Contributions of the $\gamma-\gamma'$ and $\delta-\delta'$ Interactions to Tri-Partite Exon Ligation. One property of the tri-partite assay described above that hindered more detailed kinetic analysis of the system was the relatively high Michaelis constant (K_m = 2.6 μM) for the ribozyme:3′ substrate E pair. We therefore searched for ways to create a more optimal 3′ substrate with a tighter binding constant. In addition to the three G:C base pairs in domain 6, 3′ substrate E was capable of forming two long-range A:U base pairs with nucleotides elsewhere in the intron—the so-called $\gamma-\gamma'$ and $\delta-\delta'$ interactions (*19*, *21*; see Figure 1A and Discussion). To determine whether these interactions contributed to 3′ substrate binding and/or exon ligation in the tri-partite assay, we tested various combinations of ribozymes and 3′ substrates having mutations at these positions. These reactions were carried out under single turnover conditions (i.e., 3′ substrate was limiting and 5′ exon and ribozyme were each 20 μM) at pH 7.5.

We first examined the effects of single mutations at the γ' and δ' positions in the 3′ substrate and the corresponding positions in the ribozyme (Figure 7). We specifically chose conservative mutations because phylogenetic comparisons have shown that the γ and γ' positions are always a purine and pyrimidine, respectively (*42*). When combined with wild-type ribozyme, both the γ'U→C and δ'A→G 3′ substrates reacted (lanes 11−12 and 16−17, respectively), but with somewhat slower kinetics (relative rates of 0.2 and 0.3, respectively) than the wild-type 3′ substrate (lanes 2−3). Only one cleavage product was observed for each mutant substrate and it corresponded to that expected for cleavage

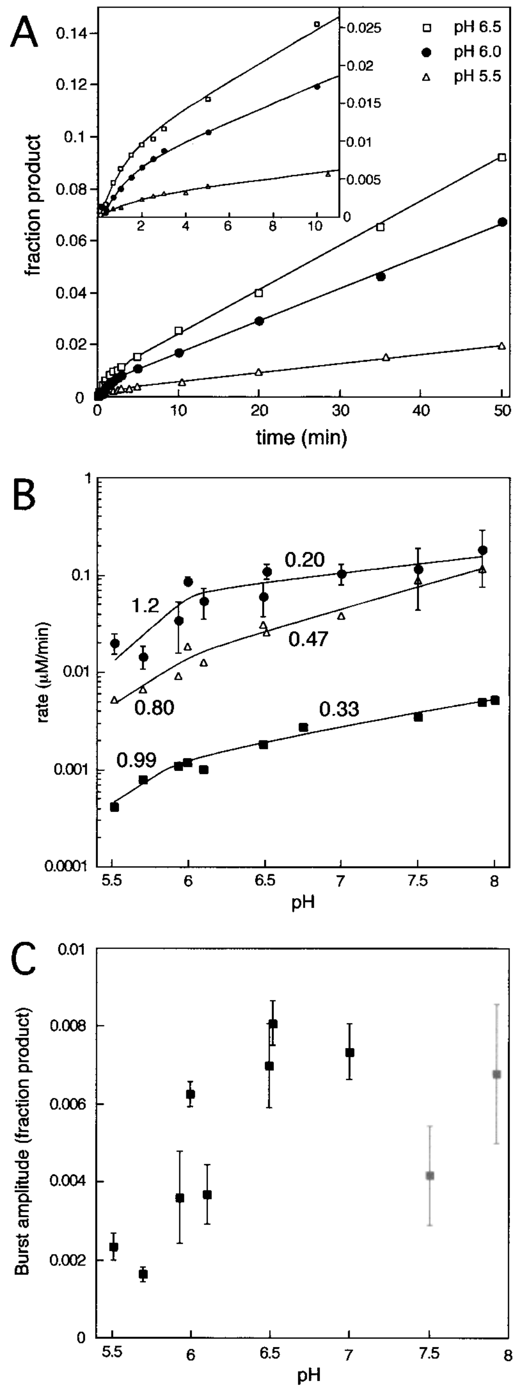

FIGURE 6: pH-rate titration of tri-partite exon ligation assay. (A) Examples of time courses (1 μM ribozyme, 15 μM 5′ exon, and 3′ substrate) at pH 6.5 (□), pH 6.0 (●), and pH 5.5 (△) show a reduction in the steady-state rate as the pH is lowered as well as a decrease in burst amplitude. The curve fits are fp = 0.000 45 + 0.0070(1 − $e^{-0.58t}$) + 0.0017t (□), fp = −0.0014 + 0.0063(1 − $e^{-0.93t}$) + 0.0012t (●), fp = −2.2 × 10^{-5} + 0.023(1 − $e^{-0.58t}$) + 0.0035t (△). (B) Dependence on pH of single (●) and multiple (△) turnover rates in the presence of an all-ribo 5′ exon or the single turnover rate (■) obtained with E1dC 5′ exon. Slopes are indicated next to the line fits. Errors from curve fitting are indicated, but are not visible on △ and ■ due to their minute size. (C) Plot of burst amplitude versus pH. Exact burst amplitudes for pHs 7.5 and 7.9 (gray) were difficult to measure, because the single and multiple turnover rates were not statistically different at these pHs (see panel B). Experiments shown here were all performed with ribozyme prepared by spin column purification (see Experimental Procedures); burst amplitudes indicate that a smaller proportion of these molecules are active compared to those prepared by gel purification.

at the natural 3′ splice site. Interestingly, a 3′ substrate containing both mutations (lanes 21−22) was also cleaved accurately between the γ' and δ' positions. However, this substrate reacted quite slowly with a relative rate of 0.01 compared to wild-type. In the converse experiment, ribozymes containing γ587A→G and δ328U→C were active and cleaved the wild-type 3′ substrate accurately (lanes 4−7), but like the above reactions, at reduced rates. The γ587A→G was significantly less active, with a relative rate of 0.05. A ribozyme containing both mutations also produced an accurate cleavage product, but displayed an intermediate reduction in rate (0.1; lanes 8−9).

We next combined the mutations in a compensatory fashion to determine if the reduced activities could be rescued by restoring the proposed base pairs. The γ587A→G ribozyme did complement the γ'U→C mutation and increased the reaction rate to 0.7 of the wild-type ribozyme:3′ substrate combination (lanes 13 and 14). In contrast, the δ328U→C ribozyme failed to improve the reaction rate of the δ'A→G 3′ substrate (lanes 18−19). Moreover, the γ587G, δ328C ribozyme only restored activity with the doubly mutated 3′ substrate up to that observed with the δ328C:δ'G pair (lanes 23−24). Thus, we were able to confirm the $\gamma-\gamma'$ interaction using the tri-partite assay, but not the δ'-δ' interaction.

Because the $\gamma-\gamma'$ G:C combination rescued the reaction rate under single turnover conditions, we determined the kinetic parameters of this ribozyme:3′ substrate pair under multiple turnover conditions. K_m and k_{cat} for this combination were 1.0 ± 0.2 μM and 0.17 ± 0.01 min^{-1}, respectively (data not shown). The $\gamma-\gamma'$ G:C base pair therefore resulted in tighter apparent substrate binding without any reduction in the steady-state rate compared to the wild-type A:U combination.

DISCUSSION

In this study, we report development of a tri-partite assay for exon ligation by the ai5γ group II intron in which the 3′ splice site is supplied by a short oligonucleotide separate from the catalytic core. Such an assay should greatly facilitate structure/function analysis of 3′ splice site recognition and exon ligation in this system. The tri-partite assay has already been used to uncover a metal ion specificity switch in the presence of a 3′ sulfur substitution at the 3′ splice site that was masked when the same modification was incorporated into a cis splicing intron (*43*). Discussed below are several aspects specific to the second step of splicing, including partial kinetic characterization of an exon ligation-specific ribozyme, tolerated structural permutations within the intron, 3′ substrate recognition elements, and activity dependence on pH.

Alternate Conformational States of the Intron. To determine an apparent binding constant for the 5′ exon in a second step assay, we monitored exon ligation rates in reactions containing free 5′ exon plus the linear intron-3′ exon splicing intermediate. These reactions exhibited distinctly biphasic kinetics (Figure 2B), similar to those observed in assays that either primarily or solely monitor the first step of splicing (Peebles, C. L., and Franzen, J. S., personal communication; *16*, *24*, *25*, *28*, *44*). In those studies, this biphasic behavior was proposed to reflect alternate conformational states of

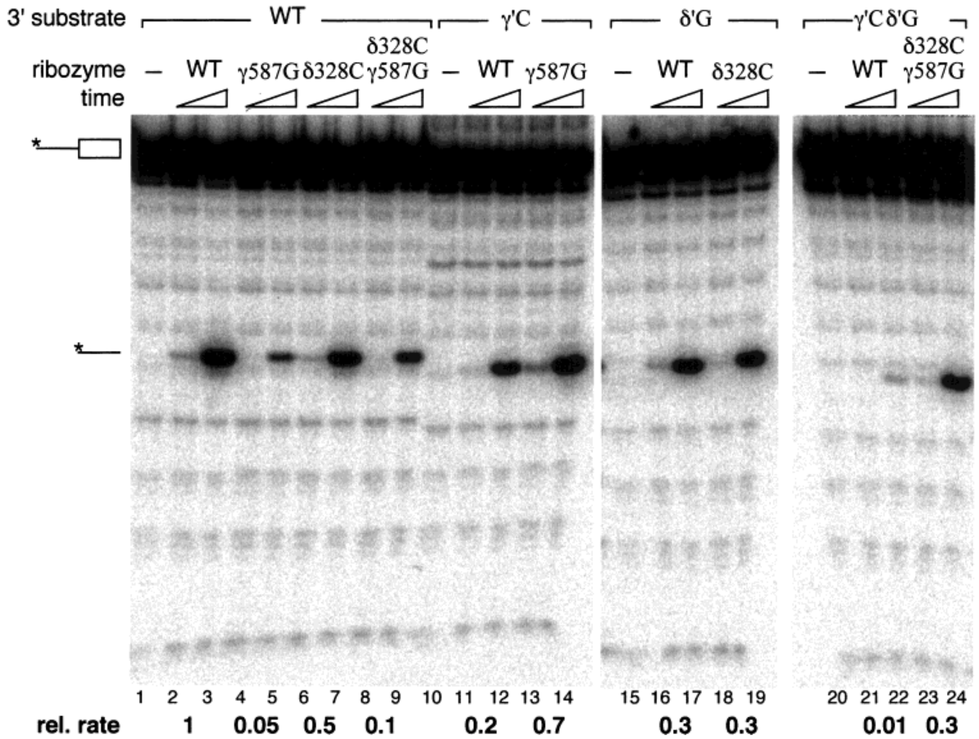

FIGURE 7: Effects of altering the $\gamma-\gamma'$ and $\delta-\delta'$ positions on tri-partite exon ligation. (A) Various combinations of singly or doubly mutated ribozymes and 3′ substrates (indicated above gel) were incubated under single turnover conditions (20 μM 5′ exon and ribozyme; 100 nM 3′ substrate; pH 7.5) for 0, 0.1, and 0.5 min. Unreacted 3′ substrate was also run on the gel (lanes 1, 10, 15, and 20). Relative rates (below gel) were calculated from the 0.5 min timepoint, known to be in the linear portion of the reaction (see Figure 5B).

the intron, but not tested. Results of a rapid denaturation/renaturation protocol using the bi-partite exon ligation assay now provide direct support for this hypothesis (Figure 2C). The alternate conformations of the intron could be either active and inactive states that slowly interconvert at 45 °C or two active states that have different reactivities and do not interconvert except at high temperature.

The most active conformer in the bi-partite exon ligation assay represented ca. 57% of the intron (Figure 2, panels B and C). Remarkably, almost identical partitioning of the two conformers was observed in the above cited studies that monitored the first step (*16*, *28*, *44*). Thus the same major conformation is likely responsible for the fast phase in both first and second step assays. Moreover, the k_{obs} for the fast phase of the bi-partite exon ligation assay (0.6 min^{-1}) was indistinguishable from the calculated single-turnover k_{obs} for the tri-partite exon ligation assay (0.7 min^{-1}). This suggests that the same active conformer is responsible for the observed rate of exon ligation in both cases. If so, then the concentration of active ribozyme in the tri-partite assay is maximally 57% of input, and the multiple turnover k_{cat} may be closer to 0.25 min^{-1} than 0.14 min^{-1}.

Rate Comparisons. Bi-partite assays similar to the one we employed here (free 5′ exon plus linear intron-3′ exon) have been described previously. Two early studies used this assay to demonstrate that exon ligation can occur independent of branching (*12*, *15*). A bi-partite assay was also used to test the effects of replacing one of the nonbridging oxygen atoms on the 3′ splice site phosphodiester with sulfur. In that study, a modified 5′ exon terminating with 2′-deoxy C (E1dC) was used to achieve conditions where chemistry might be rate limiting. The rates of exon ligation (not explicitly stated in the text) ranged from ca. 0.002 min^{-1} at pH 6 to ca. 0.05 min^{-1} at pH 7.3 (*28*). A lariat intermediate has also been used to catalyze exon ligation. In that study, a rate of ca. 1 min^{-1} was reported for reaction of an all ribose 5′ exon at pH 5.2 (*29*). None of these studies, however, reported detailed kinetic characterization of the reaction under optimal splicing conditions for the full-length intron.

The rate of branch formation catalyzed by the full-length wild-type ai5γ group II intron has been reported to be 0.22 min^{-1} under similar reaction conditions to those employed here [pH 7.5, 0.5 M $(NH_4)_2SO_4$ (*16*)]. When splicing is performed in 0.5 M KCl, which promotes 5′ splice site hydrolysis, the rate of 5′ splice site cleavage is 0.04 min^{-1} (*16*). Splicing intermediates generally do not accumulate under either condition (*7*, *8*, *15*, *20*), indicating that exon ligation must be considerably faster than either branch formation or 5′ splice site hydrolysis. The k_{obs} for a single round of exon ligation by the linear intron that we measured (0.6−0.7 min^{-1}) can readily account for the lack of intermediate accumulation in the hydrolysis pathway using full-length constructs.

Dependence of Rate on pH. In this study, we were unable to establish assay conditions in which the nature of the rate-limiting step is known. However, we did examine the effects of pH on both the bi-partite and tri-partite assays. It had previously been reported that the rates of several reactions catalyzed by group II introns (e.g., branching, reverse branching, and 5′ splice site hydrolysis, see Figure 1B) decrease with pH and become log-linear with slopes near 1.0 between pH 5 and pH 6 (*28*, *29*, *36*). This is the behavior expected if a step involving a proton transfer, such as a chemical reaction, becomes rate-limiting at low pH (*39*). Two of the above studies also examined the pH dependence of exon ligation mediated by either a linear or lariat intron-3′

exon intermediate. In both studies, a 5′ exon terminating with a 2′-deoxy-C (E1dC) was employed to decrease the rate of exon ligation. Log-linear rates with slopes near 1.0 were again observed between pH 5 and 6 (*28*, *29*).

An advantage of the tri-partite exon ligation assay is that both single and multiple turnover kinetics can be monitored simultaneously. Since the multiple turnover k_{cat} (0.14 min^{-1}) is slower than the single turnover k_{obs} (0.6−0.7 min^{-1}), it is also possible to observe burst kinetics. Under conditions where all substrates are saturating and in excess of ribozyme, an initial fast phase (the burst) represents product generated by the first turnover. The amplitude of this phase is a direct measure of active ribozyme concentration. The subsequent slower phase monitors the steady-state rate.

Similar to the above reports, we observed that the single and multiple turnover rates of exon ligation in the tripartite assay both decreased with pH (Figure 6B). At all pHs tested, however, an initial burst was clearly observable (Figure 6A). This minimally indicates that even at the lowest pH tested, the multiple turnover rate-limiting step cannot be chemistry, since this rate was invariably slower than the burst rate. Possibly indicative of rate-limiting chemistry, the rate of a single turnover did display a log-linear dependence on pH with a slope near 1 below pH 6.0. This same trend was observed with the E1dC 5′ exon. Consistent with previous reports (*28*, *29*), this modification decreased the single-turnover exon ligation rate by almost 2 orders of magnitude at all pHs, and this slow rate exhibited log-linearity with a slope of 0.99 in the 5.5−6.0 pH range. Because the E1dC rate was so slow, however, only a fraction of the first turnover could be monitored with this modified substrate, and as a result, no burst kinetics were observed.

Unexpectedly, the burst amplitude in the all-ribo reactions also displayed a distinct pH dependence below pH 6.0 (Figure 6C). Thus, lowering the pH apparently decreased the concentration of active ribozyme. Such a loss in activity could result from conversion of the ribozyme into an unfavorable conformation for catalysis (e.g., an un- or misfolded state) or an increase in either substrate binding constant. Therefore, in the tri-partite assay, the log-linear relationship between the single turnover rate and pH below pH 6 more likely results from loss of ribozyme activity than from a shift to rate-limiting chemistry. This conclusion is supported by the observation that the multiple turnover rate also displayed a log-linear pH relationship with a slope near 1 below pH 6, even though this rate is clearly not limited by chemistry (see above). In light of this observation, perhaps greater caution should be taken in interpreting pH-rate profiles, particularly when monitoring extremely slow rates where the end point of the reaction cannot be readily determined (as, for example, with the E1dC 5′ exon in a bi-partite exon ligation assay at low pH).

Effects of Domain 6 Modifications on Exon Ligation. Domain 6 plays a critical role in splicing via the branching pathway, providing the adenosine required for branch formation. Although not as conserved phylogenetically as domain 5 (*45*), domain 6 does maintain the bulged branch point and several conserved purine and pyrimidine positions (*46*). A previous study showed that elimination of the bulged branch site, by either deletion or introduction of an additional U opposite the branch site A, had no detectable effect on exon ligation (*44*). Complete deletion of domain 6 also allowed exon ligation in a cis construct, but with markedly reduced efficiency and 3′ splice site fidelity (*22*). Consistent with these results, we found that the natural domain 6 structure was not essential for accurate exon ligation in our tri-partite assay. Neither a nick in the phosphodiester backbone nor introduction of extra nucleotides had any effect on 3′ splice site fidelity (Figure 3, panels A and B and data not shown). Moreover, accurate 3′ splice site cleavage was obtained (albeit at a significantly reduced rate) when domain 6 was reduced to just three base pairs (Figure 4B and data not shown).

The only site in domain 6 of ai5γ previously shown to specifically affect exon ligation is the GUAA tetraloop. A detailed study using modification interference identified an interaction between this tetraloop (η') and two G:C base pairs in domain 2 (η; Figure 1A). Disruption of this interaction inhibited exon ligation but not 5′ splice site cleavage. Thus it was concluded that the $\eta-\eta'$ interaction is important for a conformational change in the intron that occurs between the first and second steps of splicing (*26*). However our observation that exon ligation can occur in the tri-partite assay in the absence of this interaction indicates that in a trans system where the first step has been bypassed, the $\eta-\eta'$ interaction is not essential.

Contributions to 3′ Splice Site Definition in the Tri-Partite Assay. A 3′ splice site substrate containing only three nucleotides from the intron was accurately cleaved in the tri-partite assay (Figure 3B; RNA H). This short substrate is not predicted to form any base pairs within domain 6. Therefore other interactions with the intron were most likely responsible for its recognition and binding. Previous studies have suggested that the nucleotides on either side of the 3′ splice site each form a long-distance Watson−Crick base pair with a partner in the intron: $\gamma-\gamma'$ (*21*) and $\delta-\delta'$ (*19*) (Figure 1A). The $\gamma-\gamma'$ interaction, between intron nucleotides A587 and U887, is required for efficient exon ligation in full-length constructs (*21*, *37*). The results of our tri-partite assays using wild-type and conservative substitution combinations at the γ and γ' positions (Figure 6) are consistent with these previous findings. The $\delta-\delta'$ interaction, between intron nucleotide U328 and the first nucleotide of the 3′ exon, had only been shown to influence splicing in the context of a domain 6 deletion (*19*); i.e., it had not been previously tested in an otherwise intact intron. Although mutation of either δ or δ' reduced the rate of exon ligation in the tri-partite assay, combining what should have been compensatory mutations did not rescue the rate. Thus, while the identities of both the δ and δ' positions contribute to the rate of tri-partite exon ligation, we have so far obtained no evidence for a base pair between them.

Remarkably, a 3′ substrate containing conservative mutations at both the γ' and δ' positions was accurately cleaved by the wild-type ribozyme, although at only 1% of the wild-type rate. This suggests that the primary contribution of the γ' and δ' nucleotides is not to define the actual 3′ splice site, but perhaps to increase overall binding affinity between the intron and the 3′ splice site region. This is supported by our finding that conversion of the $\gamma-\gamma'$ interaction from a A:U to a G:C base pair resulted in a 2.6-fold reduction in the 3′ splice site substrate K_m. Future studies in which the nature of the rate-limiting steps are determined for the tri-partite assay should allow a more complete analysis of the contributions of specific functional groups to binding and chemistry.

ACKNOWLEDGMENT

The authors would like to thank Lizbeth Hedstrom and Klemens Hertel for discussion of kinetics analyses; Alain Jacquier and Anna Pyle for plasmids; Alain Jacquier for sharing the template for Figure 1A; and Jeff Gelles, Lizbeth Hedstrom, Melissa Jurica, Janice Kranz and Vienna Reichert for critical reading of the manuscript. M.J.M. is an assistant investigator with the Howard Hughes Medical Institute.

REFERENCES

1. Michel, F., Jacquier, A., and Dujon, B. (1982) *Biochimie 64*, 867−881.
2. Michel, F., and Dujon, B. (1983) *EMBO J. 2*, 33−38.
3. Ferat, J.-L., and Michel, F. (1993) *Nature 364*, 358−361.
4. Maschhoff, K. L., and Padgett, R. A. (1993) *Nucleic Acids Res. 21*, 5456−5462.
5. Moore, M. J., and Sharp, P. A. (1993) *Nature 365*, 364−368.
6. Padgett, R. A., Podar, M., Boulanger, S. C., and Perlman, P. S. (1994) *Science 266*, 1685−1688.
7. Peebles, C. L., Perlman, P. S., Mecklenburg, K. L., Petrillo, M. L., Tabor, J. H., Jarrell, K. A., and Cheng, H.-L. (1986) *Cell 44*, 213−223.
8. van der Veen, R., Arnberg, A. C., Horst, G. v. d., Bonen, L., Tabak, H. F., and Grivell, L. A. (1986) *Cell 44*, 225−234.
9. Cech, T. R. (1986) *Cell 44*, 207−210.
10. Sharp, P. A. (1985) *Cell 42*, 397−400.
11. Schmelzer, C., and Schweyen, R. J. (1986) *Cell 46*, 557−565.
12. Jarrell, K. A., Peebles, C. L., Dietrich, R. C., Romiti, S. L., and Perlman, P. S. (1988) *J. Biol. Chem. 7*, 3432−3439.
13. Jarrell, K., Dietrich, R. C., and Perlman, P. A. (1988) *Mol. Cell. Biol. 8*, 2361−2366.
14. Podar, M., Perlman, P. S., and Padgett, R. A. (1995) *Mol. Cell Biol. 15*, 4466−4478.
15. Jacquier, A., and Rosbash, M. (1986) *Science 234*, 1099−1104.
16. Daniels, D. A., Michels, W. J., and Pyle, A. M. (1996) *J. Mol. Biol. 256*, 31−49.
17. Perlman, P. S., and Podar, M. (1996) *Methods Enzymol. 264*, 66−99.
18. Jacquier, A. (1996) *Biochimie 78*, 474−487.
19. Jacquier, A., and Jacquesson-Breuleux, N. (1991) *J. Mol. Biol. 219*, 415−428.
20. Jacquier, A., and Michel, F. (1987) *Cell 50*, 17−29.
21. Jacquier, A., and Michel, F. (1990) *J. Mol. Biol. 213*, 437−447.
22. Koch, J. L., Boulanger, S. C., Dib-Hajj, S. D., Hebbar, S. K., and Perlman, P. S. (1992) *Mol. Cell. Biol. 12*, 1950−1958.
23. Michels, W. J., and Pyle, A. M. (1995) *Biochemistry 34*, 2965−2977.
24. Chin, K., and Pyle, A. M. (1995) *RNA 1*, 391−406.
25. Boulanger, S. C., Faix, P. H., Yang, H., Zhuo, J., Franzen, J. S., Peebles, C. L., and Perlman, P. S. (1996) *Mol. Cell Biol. 16*, 5896−5904.
26. Chanfreau, G., and Jacquier, A. (1996) *EMBO J. 15*, 3466−3476.
27. Podar, M., Chu, V. T., Pyle, A. M., and Perlman, P. S. (1998) *Nature 391*, 915−918.
28. Podar, M., Perlman, P. S., and Padgett, R. A. (1998) *RNA 4*, 890−900.
29. Deme, E., Nolte, A., and Jacquier, A. (1999) *Biochemistry 38*, 3157−3167.
30. Melton, D. A., Kreig, P. A., Rebagliatti, M. R., Maniatis, T., and Green, M. R. (1984) *Nucleic Acids Res. 12*, 7035−7056.
31. Chabot, B. (1994) in *RNA Processing, Vol. I: A Practical Approach* (Higgins, S. J., and Hames, B. D., Eds.) pp 1−30, IRL Press, Oxford.
32. Moore, M. J., and Query, C. C. (1998) in *RNA: Protein Interactions, a Practical Approach* (Smith, C. W. J., Ed.) pp 75−108, Oxford University Press, Oxford.
33. Milligan, J. F., and Uhlenbeck, O. C. (1989) *Methods Enzymol. 180*, 51−62.
34. Enright, C., and Sollner-Webb, B. (1994) in *RNA Processing* (Higgins, S. J., and Hames, B. D., Eds.) pp 135−171, IRL Press, Oxford.
35. Liu, Q., Green, J. B., Khodadadi, A., Haeberli, P., Beigelman, L., and Pyle, A. M. (1997) *J. Mol. Biol. 267*, 163−171.
36. Pyle, A. M., and Green, J. B. (1994) *Biochemistry 33*, 2716−2725.
37. Draper, D. E., White, S. A., and Kean, J. M. (1988) *Methods Enzymol. 164*, 221−237.
38. Milligan, J. F., Groebe, D. R., Witherell, G. W., and Uhlenbeck, O. C. (1987) *Nucleic Acids Res. 15*, 8783−8798.
39. Viola, R. E., and Cleland, W. W. (1978) *Biochemistry 17*, 4111−4117.
40. Johnson, K. A. (1986) *Methods Enzymol. 134*, 677−705.
41. Herschlag, D., and Khosla, M. (1994) *Biochemistry 33*, 5291−5297.
42. Michel, F., and Jacquier, A. (1987) *Cold Spring Harbor Symp. Quant. Biol. 52*, 201−212.
43. Sontheimer, E. J., Gordon, P. M., and Piccirilli, J. A. (1999) *Genes Dev. 13*, 1729−1741.
44. Chu, V. T., Liu, Q., Podar, M., Perlman, P. S., and Pyle, A. M. (1998) *RNA 4*, 1186−202.
45. Michel, F., Umesono, R., and Ozeki, H. (1989) *Gene 82*, 5−30.
46. Michel, F., and Ferat, J.-L. (1995) *Annu. Rev. Biochem. 64*, 435−461.

BI000808W